2013 IEEE/RSJ International Conference on
Intelligent Robots and Systems (IROS)
November 3-7, 2013. Tokyo, Japan

Pop-up Assembly of a Quadrupedal Ambulatory MicroRobot

Andrew T. Baisch and Robert J. Wood
Harvard University, School of Engineering and Applied Sciences, Cambridge, MA, USA

***Abstract*— Here we present the design of a $1.27g$ quadrupedal microrobot manufactured using "Pop-up book MEMS"; the first such device capable of locomotion. Implementing pop-up assembly techniques enables manufacturing of the robot's exoskeleton and drivetrain transmissions from a single 23-layer laminate. Its demonstrated capabilities include payload capacity greater than $1.35g$ (106% of body mass), maneuverability on flat terrain, and high-speed locomotion up to $37cm/s$. Additionally, locomotion performance is compared to a hand-assembled quadruped with similar design parameters. The results demonstrate that the pop-up manufacturing methodology enables more complex mechanisms while simultaneously increasing performance over hand-assembled alternatives.**

I. Introduction

Exemplary locomotion capabilities in insects such as rapid dynamic running [1], robustly navigating rough terrain [2], and scaling vertical and inverted surfaces [3], have motivated the designs of dynamic terrestrial robots. The state of the art in small-scale legged robots includes a centipede-inspired millirobot [4], DASH [5], RHEx [6], Sprawl [7], and Raibert's running and hopping robots [8]. In addition to high-speed dynamic locomotion, these robots have demonstrated capabilities such as traversing granular media [9][10] and climbing [11][12].

The Harvard Ambulatory MicroRobot (HAMR) [13][14][15] is a sub-$2g$ robotic platform that is similarly inspired by biological principles, but manufactured at the scale of insects using the Printed Circuit MEMS (PC-MEMS) fabrication paradigm [16]. Previous work focused on the challenges of instantiating millimeter-scale actuators and multiple-DOF mechanisms in HAMR2 [14], and high-voltage power and control electronics in HAMR3 [15].

When compared to insects and other legged robots, the HAMR prototypes have only demonstrated slow, quasi-static locomotion performance; the fastest recorded speed of HAMR3 was $4.3cm/s$ (0.9 body lengths per second) on perfectly flat ground, compared to speeds up to $1.5m/s$ (50 body lengths per second) in cockroaches [1] and $2.7m/s$ (27 body lengths per second) in VelociRoach [17]. Therefore, a new class of Harvard Ambulatory MicroRobot has been developed: the HAMR-V robots in Figure 1, with the goal of achieving high-speed locomotion comparable to cockroaches and other legged robots.

Here we present the design of HAMR-V Pop-up (HAMR-VP), a $1.27g$ quadrupedal microrobot whose design implements assembly techniques inspired by pop-up books to reduce manufacturing complexity and improve locomotion performance. Pop-up assembly is a new advancement in PC-MEMS manufacturing, first demonstrated in [16]. It has since enabled the creation of complex miniature devices, such as a flapping-wing microrobot (the Monolithic Bee [18]), by reducing or eliminating difficult and tedious hand-assembly. In addition, when using pop-up assembly, tolerances are imposed by the PC-MEMS fabrication process $(1 - 10\mu m)$ rather than a much larger variance due to the limitations of human assembly. A primary goal of implementing pop-up assembly in the HAMR robot is to exploit the enhanced assembly tolerances to improve robot performance. Furthermore, simplifying manufacturing should make HAMR faster and easier to build, and therefore more accessible as a research platform.

Fig. 1. The Harvard Ambulatory MicroRobot V series of quadrupeds includes the manually assembled $1.07g$ HAMR-V (right), pop-up assembled $1.27g$ HAMR-VP (left) and $270mg$ scaled HAMR-VP (middle).

In addition to the pop-up assembled HAMR-VP, a hand-assembled version of HAMR-V was built for a comparative analysis. In Section V, results from low-speed quasi-static locomotion trials of HAMR-V and HAMR-VP are presented to identify the effects of pop-up assembly on mechanism performance. Additionally, initial high-speed performance of HAMR-VP is demonstrated. Analyzing and optimizing high-speed performance requires detailed studies of gait mechanics and compliant leg designs, which are the subject of future work.

II. Robot Morphology and Powertrain Design

HAMR-V and HAMR-VP are nearly identical in morphology, powertrain design, and parameter selection. A quadrupedal design has been chosen to reduce manufacturing complexity over earlier HAMR prototypes, while still enabling dynamic locomotion. This choice is motivated by rapidly running insects such as cockroaches, which use quadrupedal (or even bipedal) gaits at high speeds [1].

978-1-4673-6357-0/13/$31.00

Although not ideal for stability, having only four legs does not preclude slow speed, quasi-static locomotion in an insect-scale robot. This is primarily due to a sprawled posture, which prevents the robot center of mass from ever falling outside of a statically-stable support region.

The HAMR flexure-based spherical five-bar (SFB) hip joint design, introduced in HAMR2 [14] and illustrated in Figure 5c, enables two degrees of freedom (DOF) per leg: a lift DOF that raises and lowers the leg in the robot's sagittal plane, and a swing DOF that provides locomotive power in the horizontal (ground) plane. The two-DOF hip joint maps decoupled inputs from two optimal energy density piezoelectric bending bimorph actuators [19] through flexure-based four-bar transmissions to a single leg. An empirical optimization of the HAMR-V powertrain selected actuator and transmission parameters illustrated in Figure 2. The sole difference between the two robots' powertrain designs is a change in HAMR-VP's swing DOF four-bar kinematics that increases stroke amplitude.

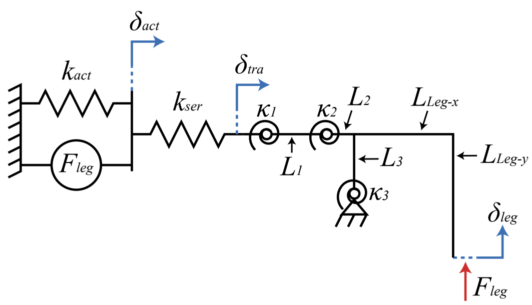

Fig. 2. Each of HAMR's leg DOFs consists of a piezoelectric actuator (force source) driving a flexure-based four-bar mechanism (linkage and torsional springs) to a leg end effector. Two decoupled inputs are mapped to each leg's orthogonal degrees of freedom, lift and swing, by a flexure-based spherical five-bar mechanism [14]. HAMR's lift DOFs are independently driven, while swing DOFs are contralaterally coupled, reducing independently driven DOFs to six.

Similarly to HAMR3 [15], design and manufacturing complexity is reduced in the HAMR-V series by asymmetrically coupling the swing DOFs of contralateral legs; when the front/rear left leg swings forward, the front/rear right leg swings rearward, and vice versa. This coupling scheme reduces the nominal eight DOFs to a total of six actuated DOFs: a front swing DOF, rear swing DOF, and four lift DOFs.

III. PC-MEMS Manufacturing

Mechanical components of HAMR-V and HAMR-VP are manufactured using the PC-MEMS (formerly SCM [20]) fabrication paradigm [16] for micron to centimeter scale systems. PC-MEMS manufacturing is characterized by creating flexure mechanisms and assembly folds by laminating alternating rigid and compliant laser-machined materials, followed by subsequent machining to release the articulated structure. This manufacturing paradigm has enabled the creation of numerous milli- and micro-robots including past generations of HAMR, a centipede-inspired millirobot [4], and the Harvard RoboBee [21].

While a diverse set of materials can be used with the PC-MEMS manufacturing process, components of the robots presented here consist of a five layer standard linkage laminate (SLL): a Kapton flexure at the laminate mid-plane, two rigid three-ply $[0, 90, 0]$ carbon fiber exterior layers (YSH-50 fibers with RS-3C resin), and two sheets of acrylic adhesive (Dupont Pyralux FR-1500) to bond subsequent layers.

A. Manufacturing and Manual Assembly of HAMR-V

Hand-assembled HAMR prototypes are made from many individual PC-MEMS components; HAMR-V has 32 parts. Each of the four SFB hip joint and transmission assemblies are constructed from four SLL components (see Figure 3). The hip assemblies are mounted to a rigid exoskeleton, comprised of four walls of four-ply $[0, 90]_s$ carbon fiber and two custom-patterned $127\mu m$ copper-clad FR4 circuit boards. Six piezoelectric actuators are soldered at their base to the two circuit boards, providing both electrical connections and mechanical ground. Actuators are affixed at their output (tip) to their respective four-bar transmission(s) using thermoplastic adhesive (Crystalbond). The powertrain is completed with four legs that attach to the output of each SFB hip.

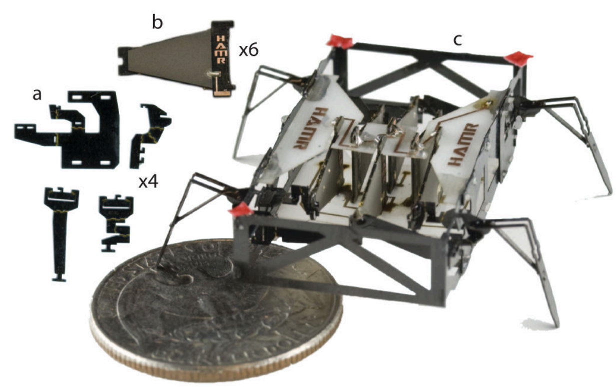

Fig. 3. Components of HAMR-V. Two Standard linkage laminate (SLL) components are manually assembled to create each spherical five-bar hip joint, and two additional components form the input four-bar transmissions (a). Mechanical power is generated by six piezoelectric bending bimorph actuators (b); four control the lift DOFs and two control swing. Additionally, four $[0, 90]_s$ carbon fiber laminates and two copper-clad FR4 circuit boards form the robot exoskeleton. All components are hand-assembled to produce the HAMR-V robot (c).

IV. Manufacturing and Assembly of HAMR-V Pop-up

Assembly tolerances of devices manufactured using the PC-MEMS process are $1-10\mu m$, driven by laser-machining and pin-alignment resolution. Therefore, prototype fidelity is highly dependent on the complexity and number of manually-assembled components. As mentioned in Section I, implementing pop-up assembly in the design of HAMR-VP is primarily motivated by the following goals: a) improving manufacturing tolerances and thus locomotion performance, and b) making the HAMR platform more accessible to other researchers by reducing manufacturing complexity. In one extreme, pop-up techniques enable complex mechanisms that emerge from a single laminate [16][18]. However unlike those devices, the HAMR-VP design does not implement a fully monolithic assembly process; it has 13 components to allow modularity of actuators and legs, two topics of concurrent research.

a) Laminate Composition: Designing HAMR-VP with pop-up assembly requires an expansion of the five-layer SLL described in Section III. The design uses 23 material layers, which compose four standard linkage sub-laminates (five layers each). Subsequent linkage sub-laminates are bonded using tack-bonded acrylic adhesive (three layers), a bonding process that enables small "islands" of adhesive rather than continuous sheets [16]. See Figure 4 for a cross-sectional view of the HAMR-VP laminate composition.

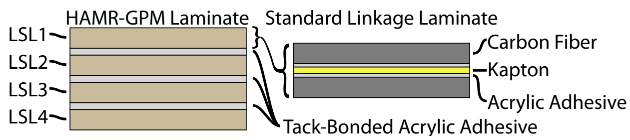

Fig. 4. The HAMR-VP laminate stack consists of 23 material layers: four standard linkage sub-laminates (five layers each) and three layers of tack-bonded adhesive to bond subsequent linkage laminates.

b) Spherical Five-Bar Sub-Laminates (LSL1 and LSL4): The pop-up HAMR-VP design utilizes the monolithic spherical five-bar joint design from [18] and [22]. This SFB design can be fabricated from a single linkage laminate, rather than from two components as in HAMR-VP (see Figure 5). Thus, manufacturing tolerances are improved and assembly is easier than described in Section III-A. Kinematically, HAMR-VP's SFB hips behave identically to those described above for HAMR-V, however each hip only requires one 90° fold to deploy the two links that couple the lift and swing DOFs. Each SFB is folded manually during final assembly of the robot, but this is trivialized by features that constrain joint limits to exactly 90°.

In the HAMR-VP material layup, two outer linkage sub-laminates labeled LSL1 and LSL4 are comprised of the four spherical five-bar hip joints. The laminate is orientated such that the robot pops-up laterally, meaning the center of the material laminate (layer 13 of 23) is also the robot sagittal midplane. Therefore, LSL1 (the robot's right side) and LSL4 (the robot's left side) are symmetric.

c) Input Four-bar and Pop-up Strut Sub-Laminates (LSL2 and LSL3): Linkage sub-laminates LSL2 and LSL3, also symmetric about the robot mid-plane, are comprised of the eight four-bar transmissions between each actuator and SFB, folding struts for popup assembly, and additional assembly features (see Figure 6). Four-bar transmissions are adhered to the SFB via tack-bonded acrylic adhesive. Each four-bar transmission is deployed with a simple 90° fold, similarly to the SFBs, and mated to its respective actuator output during final assembly.

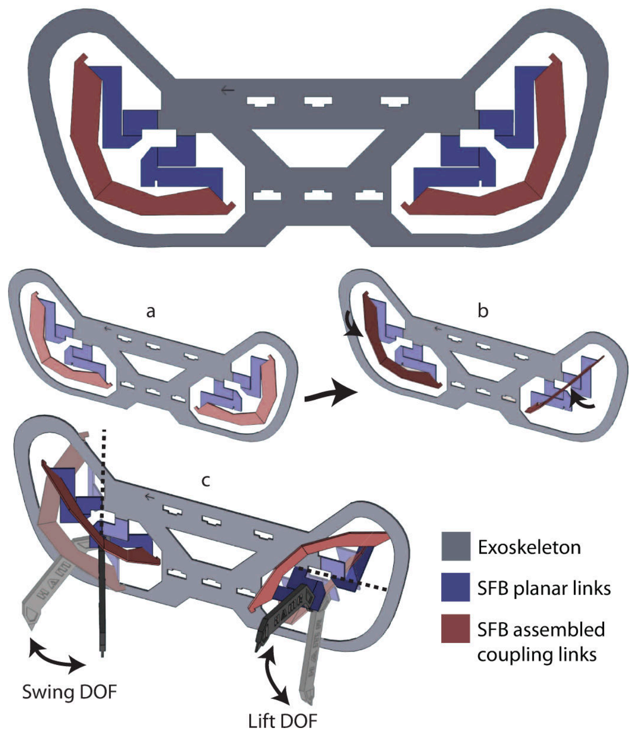

Fig. 5. HAMR-VP uses a monolithic spherical five-bar (SFB) hip joint design introduced in [18]. The outer linkage sub-laminates of HAMR-VP, LSL1 and LSL4, are composed of the four SFBs. Here, LSL4 and its two SFBs are shown as a flat laminate (a), after deployment by a 90° fold (b), and with two legs to diagram the lift and swing DOFs (c).

Three parallel assembly struts enable pop-up assembly of HAMR-VP by allowing separation of the right (LSL1 and LSL2) and left (LSL3 and LSL4) halves of the robot in a single DOF (see Figure 6). The assembly struts form a Sarrus linkage, constraining the pop-up motion such that LSL1 and LSL4 remain parallel and traverse a straight line during assembly. The robot is deployed when the assembly struts become fully extended and are orthogonal to LSL1 and LSL4. Each strut is fixed on either end to the outer linkage sub-laminates (LSL1 to LSL2 and LSL4 to LSL3), and at the laminate mid-plane (LSL2 to LSL3) using tack-bonded acrylic adhesive.

d) Laminate Manufacturing Process: The manufacturing process for HAMR-VP (see Figure 7) begins by machining the 23 material layers using a diode-pumped solid state (DPSS) laser, followed by pin-alignment and stacking on a jig. The laminate is cured under heat and pressure, then the robot outline and pop-up DOF are released from the surrounding material using the DPSS laser.

e) Final Assembly: Once released, completion of HAMR-VP requires manual assembly of the 13 components (see Figure 8). First, the exoskeleton is completed by fully expanding the pop-up DOF and inserting two copper-clad FR4 circuit boards, which trace off-board power and control electronics to the actuators. The circuit boards are populated with six piezoelectric cantilever actuators, using solder as a mechanical and electrical interface. Each input four-bar

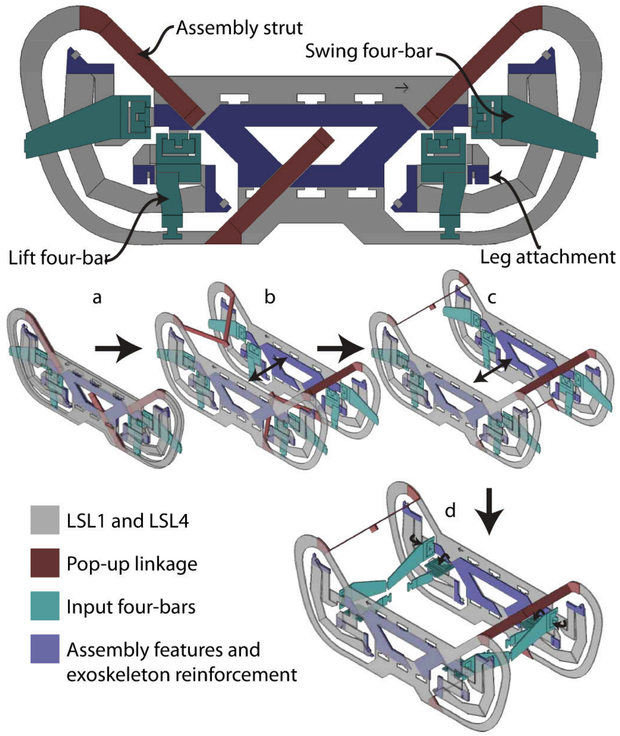

Fig. 6. Sub-laminates LSL2 and LSL3 comprise the pop-up assembly linkages, four-bar transmissions, and additional assembly features. The released pop-up linkage assembly (a) allows separation of the two robot halves (b,c), LSL1 and LSL4. After pop-up assembly, the eight input four-bars are deployed by $90°$ folds (d).

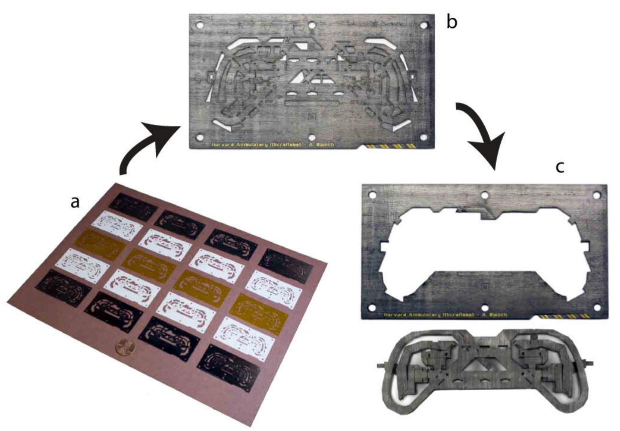

Fig. 7. Manufacturing process for the pop-up HAMR-VP. 23 material layers, 20 continuous sheets (a) and 3 tack-bonded adhesive layers, are laser machined and laminated to produce (b). A second laser-machining step releases the HAMR-VP structure (c), allowing initial pop-up assembly.

transmission is then assembled by making a $90°$ fold and affixing its input link to the output (tip) of its respective actuator. The robot is completed once spherical five-bar coupling links are folded $90°$ to their joint stop, and four legs are attached to the hip joints. As previously mentioned, legs and actuators are modular, and therefore the leg-to-hip and actuator-to-four-bar bonds are made using a thermoplastic adhesive. All other bonds, such as at $90°$ transmission folds, are made with permanent cyanoacrylate glue.

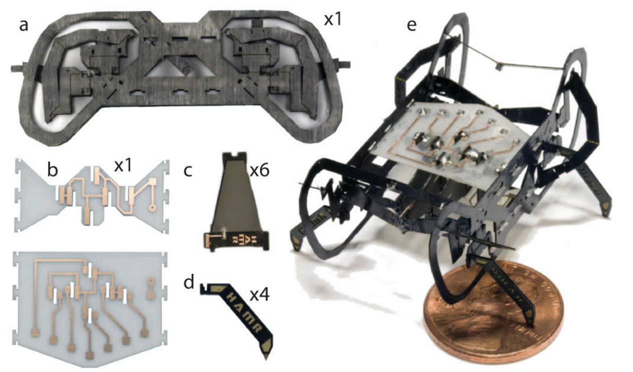

Fig. 8. The HAMR-VP pop-up laminate (a) is fully opened and constrained with two copper-clad FR4 circuit boards (b). The circuit boards, which trace from off-board power and control electronics, are populated with piezoelectric actuators (c) using solder for electrical and mechanical connection. Four-bar transmissions and SFBs are deployed, followed by attaching four legs (d) to their respective SFB output to finalize assembly of HAMR-VP (e).

V. Results

HAMR-VP was successfully manufactured, making it the the first mechanism capable of locomotion made using PC-MEMS with pop-up assembly. To evaluate the hypothesis that performance would improve with tighter assembly tolerances (attributed to popup assembly), a manually-assembled HAMR-V was fabricated for a comparative analysis of locomotion performance. As stated in Section II, the robots only differ slightly in swing-DOF kinematics. In addition, the robots differ in mass ($1.07g$ in HAMR-V and $1.27g$ in HAMR-VP) due to the additional material in the HAMR-VP laminate required to instantiate a pop-up design.

Although HAMR-VP was designed to be a high-speed, dynamic robot, it is capable of quasi-static locomotion on flat ground. Extensive high-speed locomotion performance analysis is a subject of ongoing work and is outside the scope of this paper. Therefore, most of the results presented here will be at low gait frequencies below $10Hz$.

A. Comparative Quasi-Static Locomotion Performance

At low gait frequencies, HAMR-V and HAMR-VP were evaluated in straight locomotion speed and energetics, maneuverability, and payload capacity. Results were obtained in the two-dimensional walking plane using overhead video from a Pixelink camera and custom postprocessing software that tracks the robot's center of mass and orientation.

Initial tests of all gait parameters in the HAMR-V robot led to selection of a low speed trotting gait; a two-beat gait where diagonal pairs of legs (i.e. front-left and rear-right or front-right and rear-left) propel the robot forward simultaneously. Due to the instability of a bipod, at low speeds the robot settles to a stable third leg during part of each step. The fastest quasi-static locomotion speeds were obtained for both robots with swing DOFs exactly $180°$ out of phase and lift DOFs beginning their descent to the ground $90°$ before their respective swing DOF begins driving rearwards.

Reported values in Figure 9 represent the forward velocity of the robot (as defined by a body-fixed coordinate frame) during straight locomotion, which ignores lateral and rotational motions. The only difference between robot trials is the input waveform used: in HAMR-V, a ramped square (trapezoidal) wave is used to generate the highest actuator force per stride, and thus highest speed. In HAMR-VP, sine wave inputs are used; trapezoidal inputs cause erratic behaviour at frequencies above $4Hz$, due to resonant frequency excitation in the powertrain (ringing) that causes each foot to strike the ground more than once per stride. Using sinusoidal inputs in HAMR-V resulted in lower speeds. The results show that HAMR-VP exceeds the velocity of HAMR-V by an average factor of 2.4 at comparable frequencies below $10Hz$. The measured variance in velocity reached a maximum factor of 3.0 at $2Hz$ and minimum of 1.2 at $4Hz$.

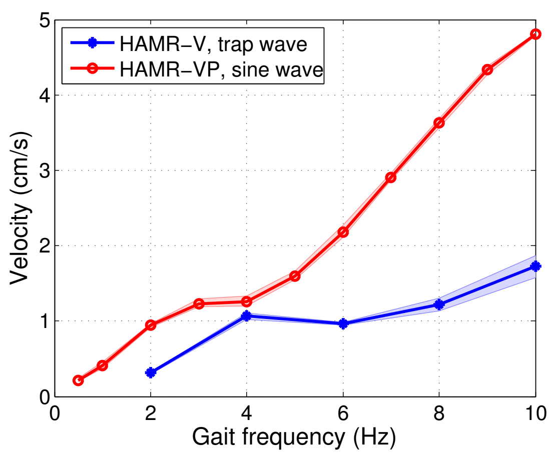

Fig. 9. Speed results from quasi-static locomotion of HAMR-V and HAMR-VP. Reported speed is the mean velocity in the direction of the robot heading, which discounts lateral drift and rotation associated with unstable quasi-static quadrupedal gaits. Error bars represent maximum and minimum speed across three trials.

Tethered, straight locomotion energetics were evaluated by measuring electrical power delivered to the six piezoelectric actuators. At trials from $0.5-10Hz$, HAMR-VP and HAMR-V required on average $11mW$ and $12mW$, respectively. Dimensionless cost of transport is commonly defined as as the work (E) required to move a weight ($M \times g$) a distance (D), or $COT = E/(M \times g \times D)$ or its equivalent $COT = P_{avg}/(V_{avg} \times M \times g)$. Due to a lower velocity and mass, HAMR-V has an average cost of transport 3.2 times greater than HAMR-VP averaged over all trials from $2 - 10Hz$.

Payload capacity was evaluated by measuring robot walking speed while carrying one to six additional $225mg$ masses (see Figure 10). On flat ground, HAMR-V failed to walk with greater than $900mg$ additional payload. HAMR-VP successfully walked with a $1350mg$ payload at speeds greater than HAMR-V with no payload.

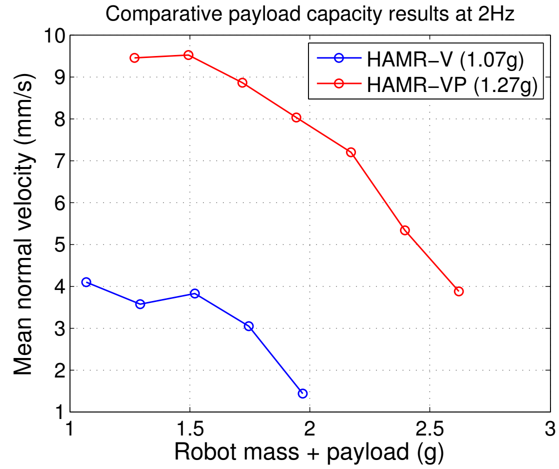

Fig. 10. Payload capacity of $1.07g$ HAMR-V and $1.27g$ HAMR-VP on flat ground. Robot velocity was measured with up to an additional $1.35g$ using discrete $225mg$ masses. At low frequencies, HAMR-V is unable to move with greater than $900mg$ of additional mass. Representative results are shown at $2Hz$ gait frequency, but were consistent from 1-10Hz.

B. Comparative Quasi-Static Trajectory Stability and Maneuverability

In related work, control schemes to turn the HAMR-V robot were investigated [23]. As a result, we determined that the simplest effective control parameter for quasi-static locomotion of the HAMR-V robots is ϕ_i ($i = 1, 2, 3, 4$), defined as the phase between a leg's lift DOF driving down to the ground, and swing DOF driving rearward to propel the robot. Increasing/decreasing ϕ_i changes the nominal foot trajectory from circular at $\phi_i = 90°$, affecting the time and duration at which leg i is driving rearward. Changing ϕ_i of only one leg introduces an asymmetry between left and right sides of the robot that causes the body to rotate.

In HAMR-V and HAMR-VP, turning was performed using ϕ_1 of the front left leg as a feedforward control parameter. Turning trajectories and final robot orientation at $2Hz$ gait frequency are presented in Figure 11 for $\phi_1 = 30, 60, 90, 120, 150$. There are various methods to quantify maneuverability during ground locomotion. Two possible metrics include average angular velocity and turning radius; higher velocity and smaller turning radius characterize faster turns. Using these metrics, HAMR-V and HAMR-VP perform nearly identically in turning rate, however HAMR-V exhibits a smaller turning radius.

Another method to measure stability in maneuverability is presented in [24], which defines a successful turn as one that simultaneously deflects average heading (the direction of average COM velocity) and changes orientation such that the robot's body axis remains aligned with its heading. In walking robots, a large variance between robot heading and orientation necessitates additional onboard sensing and control for successful turns. At HAMR-V's scale, additional components come at a large cost to payload and power. Across all trials in Figure 11, HAMR-VP outperformed HAMR-V with average heading-to-orientation deviations of

11° to 29°, respectively.

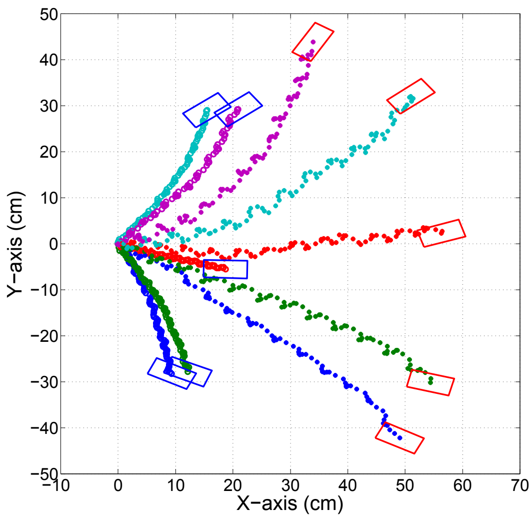

Fig. 11. Maneuverability results using ϕ_1 as a feedforward control input at $2Hz$ gait frequency over $6s$ trials. Robot trajectories are presented for $\phi_1 = 30°$ (hard right turn), $\phi_1 = 60°$ (shallow right turn), $\phi_1 = 90°$ (straight), $\phi_1 = 120°$ (shallow left turn), and $\phi_1 = 150°$ (hard left turn). The robot's orientation at the end of each trial is represented by a blue (HAMR-V) or red (HAMR-VP) rectangle.

C. HAMR-V High-Speed Locomotion Performance

Characterization of high-speed locomotion performance is outside the scope of this work, however preliminary results in Figure 12 show HAMR-VP reaching 37 cm/s (8.4 body lengths per second). Maximum speeds were obtained using gait frequencies up to 70 Hz, enabled by HAMR's high bandwidth and quality factor powertrain. The results demonstrate that using large bandwidth piezoelectric actuators enables high speed locomotion simply by increasing stride frequency, as opposed to implementing dynamic elements in the robot drivetrain (such as in other walking robot designs [5][6][7][8]). This is not to discredit the use of dynamic elements, which will be implemented in future versions of HAMR to improve efficiency and performance.

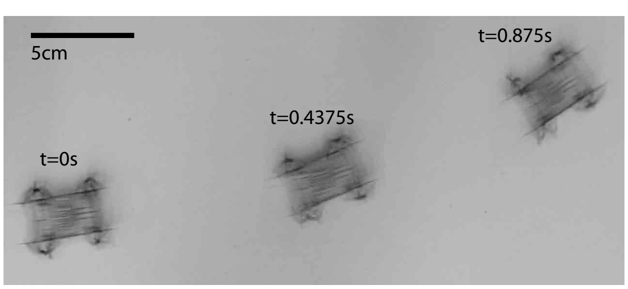

Fig. 12. By exploiting HAMR-VP's high bandwidth and quality factor powertrain, speeds up to 37 cm/s (8.4 body length per second) have been achieved using gait frequencies up to 70Hz.

D. Design Scaling

A primary goal of implementing pop-up assembly in HAMR was to make the platform more accessible to other researchers. Evaluating the success of HAMR-VP in this regard is impossible in the short term. However, a similar metric is whether the implementation of pop-up assembly enables instantiation of designs too-small or complex for manual assembly. Therefore, a smaller version of HAMR-VP was created by photographically scaling its two-dimensional CAD drawings by a factor of 0.5. The result is a $270mg$ quadruped capable of tethered, flat-ground locomotion (see Figure 1).

VI. Analysis, Conclusions, and Future Work

The design of HAMR-VP, a $1.27g$ quadrupedal microrobot manufactured using the PC-MEMS fabrication paradigm and pop-up assembly techniques, has been presented here. Locomotion studies were performed on HAMR-VP to evaluate it as a miniature robotic platform. Furthermore, to quantify the effect of implementing pop-up assembly into a HAMR design, quasi-static locomotion results were compared to HAMR-V, a $1.07g$ hand-assembled robot with nearly identical design parameters. The results of this comparison suggest that designing HAMR for pop-up assembly improved walking speed, efficiency, payload, and maneuverability.

In quasi-static straight line speed trials from $1 - 10Hz$, HAMR-VP outperformed HAMR-V by an average factor of 2.4 across comparable gait frequencies. Due to HAMR-V's lower mass and speed but similar power requirements, its average cost of transport was 3.2 times greater than HAMR-VP. Although the increase in velocity can partially be attributed to a change in swing-DOF kinematics, an improvement in flat-ground payload capacity suggests that despite identical design parameters, HAMR-VP has a greater power output in the lift DOF. In maneuverability trials, HAMR-V and HAMR-VP demonstrated similar turning rates, however HAMR-VP showed significantly better performance in turn stability. In order to validate the claim that using pop-up assembly improves mechanism performance, a direct comparison of leg force and displacement outputs should be performed for the pop-up and hand-assembled robots.

A $270mg$ quadruped capable of tethered flat ground locomotion was also presented here. This robot, along with other work [16][18][22], demonstrate a variety of complex miniature devices achievable only by implementing pop-up assembly into PC-MEMS manufactured devices. With the locomotion performance results presented here, we have shown that implementing pop-up assembly into PC-MEMS devices simultaneously improves mechanism performance and increases achievable mechanism complexity.

Within the Harvard Microrobotics Lab, HAMR-VP is now a platform for additional research in a variety of fields. Current work includes implementation of onboard electronics similar to HAMR3 [15], feedback control using onboard sensing, and modifying feet and actuator signals to obtain a desirable operating point for dynamic locomotion.

Acknowledgments

The authors gratefully acknowledge the Wyss Institute for Biologically-Inspired Engineering (Harvard University) and the ARL Micro Autonomous Systems and Technology (MAST) program for their support of this work. Harvard Microrobotics Lab members Onur Ozcan and Dani Ithier are also thanked for their valuable contributions to the HAMR project. Author Andrew Baisch would like to thank the Department of Defense for their support through the National Defense Science & Engineering Graduate Fellowship (NDSEG) program.

References

[1] R. Full and M. Tu, "Mechanics of a rapid running insect: two-, four- and six-legged locomotion," *J. of Experimental Biology*, vol. 156, pp. 215–231, 1991.

[2] S. Sponberg and R. Full, "Neuromechanical response of musculo-skeletal structures in cockroaches during rapid running on rough terrain," *J. of Experimental Biology*, vol. 211, pp. 433–446, May 2008.

[3] D. Goldman, T. Chen, and D. Dudek, "Dynamics of rapid vertical climbing in cockroaches reveals a template," *J. of Experimental Biology*, vol. 209, no. 15, p. 2990, 2006.

[4] K. Hoffman and R. Wood, "Turning gaits and optimal undulatory gaits for a modular centipede-inspired millirobot," in *4th IEEE RAS/EMBS Conf. on Biomedical Robotics and Biomechatronics (BioRob)*, Rome, Italy, 2012, pp. 1052–1059.

[5] P. Birkmeyer, K. Peterson, and R. Fearing, "DASH: A dynamic 16g hexapedal robot," in *IEEE/RSJ Intl. Conf. on Intelligent Robots and Systems*, St. Louis, MO, 2009, pp. 2683–2689.

[6] U. Saranli, M. Buehler, and D. Koditschek, "RHex - a simple and highly mobile hexapod robot," *Intl. J. of Robotics Research*, vol. 20, pp. 616–631, Jul. 2001.

[7] S. Kim, J. Clark, and M. Cutkosky, "iSprawl: Design and tuning for high-speed autonomous open-loop running," *Intl. J. of Robotics Research*, vol. 25, no. 9, pp. 903–912, 2006.

[8] M. Raibert, *Legged robots that balance*. The MIT Press, Cambridge, MA, 1985.

[9] C. Li, P. Umbanhowar, H. Komsuoglu, D. Koditschek, and D. Goldman, "Sensitive dependence of the motion of a legged robot on granular media," *Proc. of the National Academy of Sciences*, vol. 106, no. 9, pp. 3029–3034, 2009.

[10] C. Li, A. Hoover, P. Birkmeyer, P. Umbanhowar, R. Fearing, and D. Goldman, "Systematic study of the performance of small robots on controlled laboratory substrates," in *SPIE Defense, Security, and Sensing Conf.*, Orlando, FL, Apr. 2010.

[11] P. Birkmeyer, A. Gillies, and R. Fearing, "Clash: Climbing vertical loose cloth," in *IEEE/RSJ Intl. Conf. on Intelligent Robots and Systems*, San Francisco, CA, 2011, pp. 5087–5093.

[12] ——, "Dynamic climbing of near-vertical smooth surfaces," in *IEEE/RSJ Intl. Conf. on Intelligent Robots and Systems*, Vilamoura, Portugal, 2012.

[13] A. Baisch and R. Wood, "Design and fabrication of the harvard ambulatory microrobot," in *14th Intl. Symp. on Robotics Research*, Lucerne, Switzerland, Sep. 2009.

[14] A. Baisch, P. Sreetharan, and R. Wood, "Biologically-inspired locomotion of a 2g hexapod robot," in *IEEE/RSJ Intl. Conf. on Intelligent Robots and Systems*, Taipei, Taiwan, 2010, pp. 5360–5365.

[15] A. Baisch, C. Heimlich, M. Karpelson, and R. Wood, "HAMR3: An autonomous 1.7g ambulatory robot," in *IEEE/RSJ Intl. Conf. on Intelligent Robots and Systems*, San Francisco, CA. USA, 2011, pp. 5073–5079.

[16] J. Whitney, P. Sreetharan, K. Ma, and R. Wood, "Pop-up book mems," *J. of Micromechanics and Microengineering*, vol. 21, no. 11, p. 115021, 2011.

[17] D. Haldane, K. Peterson, F. G. Bermudez, and R. Fearing, "Animal-inspired design and aerodynamic stabilization of a hexapedal millirobot," in *IEEE Intl. Conf. on Robotics and Automation*, Karlsruhe, Germany, 2013.

[18] P. Sreetharan, J. Whitney, M. Strauss, and R. Wood, "Monolithic fabrication of millimeter-scale machines," *J. of Micromechanics and Microengineering*, vol. 22, no. 5, p. 055027, 2012.

[19] R. Wood, E. Steltz, and R. Fearing, "Optimal energy density piezoelectric bending actuators," *J. of Sensors and Actuators A: Physical*, vol. 119, no. 2, pp. 476–488, 2005.

[20] R. Wood, S. Avadhanula, R. Sahai, E. Steltz, and R. Fearing, "Microrobot design using fiber reinforced composites," *J. of Mechanical Design*, vol. 130, p. 052304, 2008.

[21] R. Wood, "The first flight of a biologically-inspired at-scale robotic insect," *IEEE Transactions on Robotics*, vol. 24, no. 2, Apr. 2008.

[22] Z. Teoh and R. Wood, "A flapping-wing microrobot with a differential angle-of-attack mechanism," in *IEEE Intl. Conf. on Robotics and Automation*, Karlsruhe, Germany, 2013.

[23] O. Ozcan, A. Baisch, and R. Wood, "Design and feedback control of a biologically inspired miniature quadruped," in *IEEE/RSJ Intl. Conf. on Intelligent Robots and Systems*, Tokyo, Japan, 2013.

[24] R. Full, T. Kubow, J. Schmitt, P. Holmes, and D. Koditschek, "Quantifying dynamic stability and maneuverability in legged locomotion," *Integrative and comparative biology*, vol. 42, no. 1, pp. 149–157, 2002.